Published in final edited form as:
Hum Mol Genet. 2006 June 15; 15(12): 2003–2014.

Inhibitors of Differentiation (ID1, ID2, ID3 and ID4) genes are neuronal targets of MeCP2 that are elevated in Rett syndrome

Sailaja Peddada, **Dag H. Yasui**, and **Janine M. LaSalle***
Medical Microbiology and Immunology, Rowe Program in Human Genetics, School of Medicine, One Shields Ave, University of California, Davis, CA, 95616, USA

Abstract

Rett syndrome (RTT) is an X-linked dominant neurodevelopmental disorder caused by mutations in *MECP2*, encoding methyl-CpG binding protein 2. MeCP2 is a transcriptional repressor elevated in mature neurons and is predicted to be required for neuronal maturation by regulating multiple target genes. Identifying primary gene targets in either *Mecp2*-deficient mice or human RTT brain has proven to be difficult, perhaps because of the transient requirement for MeCP2 during neuronal maturation. In order to experimentally control the timing of MeCP2 expression and deficiency during neuronal maturation, human SH-SY5Y cells undergoing mature neuronal differentiation were transfected with methylated MeCP2 oligonucleotide decoy to disrupt the binding of MeCP2 to endogenous targets. Genome-wide expression microarray analysis identified all four known members of the inhibitors of differentiation or inhibitors of DNA binding (*ID1*, *ID2*, *ID3* and *ID4*) subfamily of helix-loop-helix (HLH) genes as novel neuronal targets of MeCP2. Chromatin immunoprecipitation analysis confirmed binding of MeCP2 near or within the promoters of *ID1*, *ID2* and *ID3*, and quantitative RT-PCR confirmed increased expression of all four *Id* genes in *Mecp2*-deficient mouse brain. All four ID proteins were significantly increased in *Mecp2*-deficient mouse and human RTT brain using immunofluorescence and laser scanning cytometric analyses. Because of their involvement in cell differentiation and neural development, ID genes are ideal primary targets for MeCP2 regulation of neuronal maturation that may explain the molecular pathogenesis of RTT.

INTRODUCTION

Rett syndrome (RTT) is an X-linked dominant disorder caused by mutation in methyl CpG binding protein 2 (*MECP2*) located on Xq28 (1,2). RTT primarily affects females, who are mosaic for expression of the *MECP2* mutation because of random X-inactivation (3). The onset of symptoms is delayed until 6–18 months of age and includes severe mental retardation with absence of speech, stereotypic hand movements, epileptic seizures and respiratory dysfunction (4–6).

MeCP2 belongs to a family of methyl-CpG-binding proteins consisting of MBD1, MBD2, MBD3 and MBD4, all of which contain a conserved methyl-CpG-binding domain (MBD) (7,8). Mice lacking MBD1 show deficits in adult neurogenesis and hippocampal function (9). Mice lacking MBD2 show mild maternal behavior deficits, while MBD3$^{-/-}$ mice die at an early embryonic stage (10). Mice deficient in MBD4, a mismatch repair enzyme, show deficits in DNA repair and increased tumor formation (11). *Mecp2*-deficient and mutant mouse models recapitulate the neurodevelopmental symptoms of RTT (12–14).

*Address correspondence to: Janine M. LaSalle, Medical Microbiology and Immunology, One Shields Ave., Davis, CA 95616, (530) 754-7598 (phone), (530) 752-8692 (fax), jmlasalle@ucdavis.edu

MeCP2, the most extensively studied member of MBD family, is a nuclear protein dynamically expressed during postnatal mammalian brain development and is a marker for neuronal maturity (15–18). Elevated MeCP2 expression is hypothesized to be required for neuronal differentiation by the regulation of multiple target genes (19). MeCP2 binds to DNA through its methyl-CpG-binding domain (MBD) and complexes with the transcriptional repressor Sin3A and histone deacetylase (HDAC) through the transcriptional repressor domain (TRD) (20–22). The involvement of MeCP2 in methylation specific transcriptional repression (20, 23) suggested that MeCP2 deficiency in RTT would result in wide spread gene dysregulation. This hypothesis was previously tested using gene expression microarray analysis with *Mecp2*-deficient mouse brain (24), RTT patient cell lines (25) and post-mortem RTT brain tissue (26). Subtle and non-overlapping transcriptional changes were observed in each of these studies, indicating that MeCP2 deficiency does not result in obvious high levels of genome-wide transcriptional dysregulation. The changes in gene expression observed due to MeCP2 deficiency in human and mouse brains could be representative of events downstream of direct MeCP2 target genes and therefore may be inherently noisy.

Alternative approaches have also been used to identify primary targets of MeCP2. In mammals, *BDNF* has been identified by a candidate gene approach (27,28) and *DLX5* was identified by cloning fragments from MeCP2 chromatin immunoprecipitation (ChIP) (29). In *Xenopus laevis*, the neuronal repressor *xHairy2a* was identified as a target of MeCP2 in differentiating neuroectoderm (30). A cDNA microarray analysis was performed on lymphoblastoid cell lines derived from RTT patients with and without MeCP2 mutations followed by ChIP to distinguish the direct targets of MeCP2 from indirect targets (31). Significantly reduced expression of *UBE3A* and *GABRB3* genes within the human 15q11-13 region in *Mecp2*-deficient mice and RTT patients was shown using multiple quantitative methods (32). Finally, a recent study demonstrated increased expression of serum glucocorticoid-inducible kinase 1 (*Sgk*) and FK506-binding protein 5 (*Fkbp5*) in *Mecp2*-deficient mouse brain suggesting MeCP2 as a modulator of glucocorticoid-inducible gene expression (33). Each of these studies identified various genes dysregulated due to MeCP2 deficiency but none of the target genes could completely explain the primary neurodevelopmental defect observed in RTT patients.

Since the phenotypic effects of MeCP2 deficiency appears to be limited to a precise stage of postnatal neuronal maturation, we used an alternative approach to experimentally control the timing of MeCP2 expression and inhibition in a neuronal cell culture system. Microarray analysis of transcriptional changes during maturational differentiation that were specifically altered by MeCP2 inhibition identified *ID1, ID2, ID3* and *ID4* genes as primary targets of MeCP2. All four ID genes belong to the same class of helix loop helix transcriptional regulators, encoding known inhibitors of differentiation or inhibitors of DNA binding that block the function of tissue specific basic helix loop helix (bHLH) transcription factors involved in regulation of important neuronal differentiation genes such as *NEUROD1*. We report significantly increased protein expression of all four ID genes in both *Mecp2*-deficient mice and RTT human brain tissue compared to wild type mice or age matched controls. Further understanding the role of ID genes as neuronal targets of MeCP2 may explain the arrest in postnatal neuronal maturation seen in Rett syndrome.

RESULTS

Microarray analysis performed to identify the primary targets of MeCP2 during SH-SY5Y differentiation

In order to identify genes specifically regulated by MeCP2 at a precise stage of neuronal maturational differentiation, expression microarray experiments were conducted on human SH-SY5Y neuronal cells transfected with a methylated oligonucleotide decoy to block MeCP2 binding to endogenous target genes during phorbol 12-myristate 13-acetate (PMA) induced

maturational differentiation. SH-SY5Y human neuroblastoma cells were chosen because they can be induced by PMA to produce a functional sympathetic neuronal phenotype (34), resulting in the two-fold increase in MeCP2 expression by 48 h (35). The MeCP2 decoy (MD) is a 22 mer double stranded DNA molecule containing two methylated CpG sites adjacent to AT-runs (36). A control sequence with CpG sites mutated to AT was used as a specificity and transfection control decoy (CD). The decoy approach of blocking MeCP2 binding in SH-SY5Y cells has been previously validated in our lab and the specificity to MeCP2 was demonstrated by ChIP at the *SNURF/SNRPN* locus (37).

Four different SH-SY5Y treatments were compared by gene expression profiling experiments: 1) Undifferentiated (**UD**) 2) 48 h differentiated and untransfected (**D-UT**) 3) 48 h differentiated and MeCP2 decoy transfected (**D-MD**), and 4) 48 h differentiated and control decoy transfected (**D-CD**). For each cell treatment, total RNA was isolated from triplicate biological experiments and labeled cRNA was hybridized to Affymetrix HG U133 plus 2.0 arrays (12 arrays in total). Data analysis was performed using dChip analysis software and significant differences between different cell treatments were identified.

As MeCP2 was hypothesized to regulate genes involved in neuronal maturation, we first chose to examine genes significantly changed following SH-SY5Y differentiation that could be potential targets of MeCP2. A Boolean logic approach was used to identify transcript levels significantly affected during differentiation by the D-MD but not the D-CD transfection. Table 1 demonstrates the pair-wise analyses that were useful in determining the genes altered specifically by the MeCP2 decoy. First, transcripts showing ≥ 2.0 or ≤ 2.0 fold significant changes ($p \leq 0.05$) between UD and D-UT are selected. PMA induced differentiation of human SH-SY5Y neuronal cells resulted in up-regulation of 183 genes and down-regulation of 45 genes compared to undifferentiated cells. Of this selected list of 228 genes, 24 genes (20 increased and 4 decreased upon differentiation) were found to have significant ($p \leq 0.05$) differences between undifferentiated and MeCP2 decoy but not undifferentiated and control decoy (UD vs. D-MD NOT D-CD). Interestingly, of the MeCP2 target candidate genes, expression levels of 3 out of 4 genes decreased with differentiation (*ID1*, *ID2*, and *ID3*) and 1 out of 12 genes increased with differentiation (*ID4*) were from the same family of transcriptional regulators called inhibitors of differentiation or inhibitors of DNA binding (ID) involved in cellular proliferation and differentiation (38,39). The fold changes and *P* values of all four ID genes from the microarray analysis are shown in Table 2 and raw data from microarray is shown in Supplementary Figure 1. The complete lists of genes from the above analysis are shown in supplementary tables S1 to S5. The simplistic pairwise analysis of D-MD versus D-CD revealed some differentially expressed transcripts (Supplementary table, S6), but because the control decoy (D-CD) had an unexpected nonspecific effect on MBD1 and MBD2 binding (37) this comparison was less informative. The microarray data discussed in this publication have been deposited in NCBIs Gene Expression Omnibus (GEO, http://www.ncbi.nlm.nih.gov/geo/) and is accessible through GEO Series accession number **GSE4600**.

The effect of MeCP2 deficiency and the binding sites for MeCP2 were further characterized for the ID gene family because of the common relationship between all four ID genes (40) and their known involvement in cellular differentiation (39,41).

Validation of ID gene expression microarray results by quantitative RT-PCR in human SH-SY5Y neuronal cells

The microarray results were confirmed by performing quantitative real time reverse transcriptase polymerase chain reaction (qRT-PCR) on all four ID genes in the SH-SY5Y MeCP2 decoy experimental system. Results shown in Figure 1A are relative fold changes compared to undifferentiated SH-SY5Y cells (UD) set at 1.0, represented by the hatched bar.

Consistent with the microarray results, qRT-PCR data for *ID1*, *ID2* and *ID3* genes showed a decrease in transcript level in differentiated SH-SY5Y cells (D-UT), but increased expression in differentiated cells transfected with MeCP2 decoy (D-MD) relative to D-UT. The *ID4* transcript levels increased following SH-SY5Y differentiation and further increased in the MeCP2 decoy (D-MD) transfected cells also compared to D-UT.

Quantitative RT-PCR of ID genes in *Mecp2*-deficient (*Mecp2*$^{tm\ 1.1Bird/y}$) mouse brain

To test the relevance of ID genes as neuronal targets of MeCP2 in a more relevant biological system, qRT-PCR was conducted using cDNA from postnatal 28, 49 and 70 day *Mecp*2$^{-/y}$ and littermate *Mecp*2$^{+/y}$ brain. Figure 1B shows the relative fold change of *Mecp*2$^{-/y}$ compared to *Mecp*2$^{+/y}$ brain cDNA (*Mecp*2$^{+/y}$ set to 1.0, hatched bar) for all four Id genes. At the youngest time point (P28), increases in *Id1* (2.5 fold), *Id2* (1.3 fold), *Id3* (1.9 fold) and *Id4* (3.5 fold) transcripts were observed in *Mecp*2$^{-/y}$ compared to *Mecp*2$^{+/y}$ brain samples. Interestingly, in the later P70 time point increased transcript levels were observed only for *Id1* in *Mecp*2$^{-/y}$ brain compared to *Mecp*2$^{+/y}$. Decreased expression levels were observed for *Id2*, *Id3* and *Id4* by P70. These results not only show the reproducibility of the microarray results using qRT-PCR in a different experimental system for inhibiting MeCP2, but also suggest that the transcriptional changes in the ID genes caused by MeCP2 deficiency may be developmental stage specific and transient.

Quantitative RT-PCR on a downstream target of ID genes in *Mecp2*-deficient mouse brain

To test the hypothesis that aberrantly increased expression of ID genes has long-lived consequences on the expression of the downstream genes important for neuronal maturation, qRT-PCR was also performed on an autoregulated bHLH transcription factor, neurogenic differentiation factor 1(*Neurod1*) (42). Figure 1C demonstrates progressive 20 % to 75 % decreased expression of *Neurod1* in *Mecp2*$^{-/y}$ brain from P28 to P70 relative to *Mecp2*$^{+/y}$ brain. It has been shown previously that ID2 in cultured HeLa and HIT cells (43) and ID2 and ID3 in *Xenopus* embryos (44) act as inhibitors of *NEUROD1* activity. These results suggest that the transient increase in ID transcript levels associated with MeCP2 deficiency could trigger a cascade of downstream events that affect postnatal neuronal maturation.

ID protein expression changes in *Mecp2*-deficient mouse model using immunofluorescence and quantitative laser scanning cytometry

Interestingly, the results from qRT- PCR data for *Mecp2*-deficient mice showed increased transcript for all four ID genes at P28. To examine and quantitate ID protein expression, immunofluorescence followed by quantitation by laser scanning cytometry (LSC) was performed for all four ID genes on P28 day sagittal brain sections of three *Mecp2*$^{tm\ 1.1Bird/y}$ mice and corresponding *Mecp2*$^{+/y}$ littermate controls. The approach of immunofluorescence on tissue microarrays and brain sections followed by analysis using LSC has been previously validated in our lab in several studies (15,32).

Briefly, immunofluorescence was performed on the 5 μm sagittal mouse tissue sections by staining the slides with each of the four ID antibodies, followed by secondary fluorescent antibody staining and detection using LSC. The fluorescently stained cells were analyzed by LSC that creates contours around the nuclei to identify individual cells. Quantitative data regarding mean fluorescence intensities (representative of total protein expression) was recorded for each cell in different fluorescent channels. Each brain region was individually gated to obtain the mean fluorescence of each ID protein. Figure 2 shows representative LSC images for all four ID protein expressions, showing differences in regional distribution in *Mecp2*$^{-/y}$ compared to *Mecp2*$^{+/y}$. Each pixel on the LSC image represents an individual cell, colored on the basis of each of the ID protein‘max pixel’ histograms of whole brain. Max pixel is the maximum fluorescence intensity of each contoured nucleus, as described previously

(15,45). Blue colored nuclei (negative) were gated based on overlap with IgG negative control histogram. Green (low) and red (high) regions were colored based on the right half max of the major peak of the ID protein max pixel histogram. Significantly increased expression of all four ID proteins was observed in multiple brain regions (cerebrum, cerebellum, thalamus and hypothalamus, medulla oblongata and pons and hippocampus) of P28 *Mecp2*$^{-/y}$ mice brain compared to *Mecp2*$^{+/y}$ littermate control. Numerical data from separately gated brain regions for all four ID proteins at time point P28 from three pairs of mice are shown in Table 3.

To determine if ID protein expression changes observed in *Mecp2*$^{-/y}$ were transient or long-lived, LSC analysis was performed on a tissue microarray consisting of cerebral cortex samples from *Mecp2*$^{-/y}$ mice and corresponding *Mecp2*$^{+/y}$ littermate controls at various developmental time points ranging from embryonic day 15 (E 15) to postnatal day 70 (P70). For each time point and ID protein, fluorescence max pixel values of cells from *Mecp2*$^{-/y}$ mouse cerebral cortex tissue cores were compared to those from *Mecp2*$^{+/y}$ cores (Table 4). The protein expression of ID1 in *Mecp2*$^{-/y}$ mouse brain showed significant increases compared to controls in E15 and in four postnatal time points (P7, P28, P49 and P70), while ID2 showed significant increases at E15 and five postnatal time points (P7, P28, P49, P56 and P70). The protein expression of ID3 increased significantly in P7, P56 and P70, while ID4 protein expression increased significantly in four postnatal time points (P28, P49, P56 and P70) of *Mecp2*$^{-/y}$ mice compared to *Mecp2*$^{+/y}$ littermate controls.

ID protein expression changes on a tissue microarray containing human RTT and control cerebral samples using immunofluorescence and quantitative laser scanning cytometry

In order to determine whether ID protein expression is also significantly higher in MeCP2 deficient RTT human brain samples, a similar approach of immunofluorescence followed by quantiation on LSC was performed. A tissue microarray containing human post-mortem cerebral cortex samples in triplicates from different RTT individuals all with known *MECP2* deficiencies (46) of different ages and corresponding age-matched control individuals was used. Figure 3 demonstrates that one male and two females with known *MECP2* deficiencies (grey, filled histograms) show significantly higher ID protein expression compared to age-matched controls (black, open histogram). Increased ID protein expression was observed in all the RTT individuals compared to controls except for ID1 in RTT 4312 brain tissue. The observed dysregulation of ID protein expression in RTT brains further supports the ID gene family as relevant neuronal targets of MeCP2 and suggests a role in the pathogenesis of RTT.

These combined results demonstrate that increased expression of the ID family of transcriptional regulators is observed in *Mecp2*-deficient mouse brain and human RTT cortical tissue. These results validate the microarray results and suggest that the novel finding of ID genes as targets of MeCP2 is not simply an artifact of the SH-SY5Y cell culture system.

Chromatin immunoprecipitation analysis of MeCP2 binding to the ID gene promoters

In order to determine whether MeCP2 binds to the CpG islands overlapping the promoter of each ID gene, ChIP was performed on chromatin isolated from SH-SY5Y cells from all four experimental conditions used for the microarray experiment (UD, D-UT, D-MD, D-CD). The specificity of the MD decoy in blocking the binding of MeCP2 to an endogenous target (*SNRPN*) has been previously validated (37), and was therefore used as a control. In Figure 4, the ChIP results for *ID1, ID2* and *ID3* show enriched binding for MeCP2 in differentiated SH-SY5Y cells (D-UT) and in the cells transfected with control decoy (D-CD). In contrast, the chromatin isolated from cells transfected with MeCP2 decoy (D-MD) or in undifferentiated cells (UD) did not show enriched binding of MeCP2. These results suggests that the down-regulation of *ID1, ID2* and *ID3* gene expression with differentiation in SH-SY5Y cells is regulated by direct binding of MeCP2 at CpG islands overlapping the promoter region of *ID1*,

ID2 and *ID3* and that MeCP2 binding is specifically reduced by MD decoy. In contrast, MeCP2 was not found to be associated with the promoter of *ID4*, suggesting that the MeCP2 may bind outside of the CpG island assayed. Alternatively, the effect of MeCP2 binding to the CpG island at the promoter may be more complex than simply repressing ID gene expression in *cis* and may instead involve long-range chromatin interactions mediated by MeCP2 as reported in a recent study (29).

DISCUSSION

MeCP2 protein levels are significantly higher in central nervous system (CNS) tissues compared to non-CNS tissues, addressing a major paradox in the pathogenesis of RTT regarding how mutations in ubiquitously transcribed *MECP2* result in a phenotype specific to the CNS (19,45). Several studies have shown that elevated MeCP2 expression is acquired during postnatal brain development, suggesting that MeCP2 might play an important role during neuronal maturation and synaptogenesis (16,17,19). In order to identify primary MeCP2 targets in the CNS and understand the cascade of events that follows their dysregulation, studying the right tissue at the right stage of differentiation is critical.

In this study we performed expression microarray analysis to identify novel gene targets of MeCP2 during neuronal maturational differentiation in a human SH-SY5Y neuronal cell culture system. MeCP2 binding to endogenous targets at a precise stage of neuronal maturational differentiation was specifically inhibited by transfection with a MeCP2 decoy. Both transcriptionally up and down regulated MeCP2 target genes have been observed by microarray analysis, consistent with previous studies (24–26), and arguing against a single role for MeCP2 as a transcriptional repressor. Using microarray analysis, we have identified all four known members of the ID subfamily of helix loop helix (HLH) proteins as novel neuronal targets of MeCP2. The microarray results reported in this study were consistent with published data showing that *ID1*, *ID2* and *ID3* transcript levels decreased upon SH-SY5Y neuronal differentiation (47) and *ID4* expression level increased following neuronal differentiation (48). Our findings are novel in demonstrating that MeCP2 regulates ID gene transcriptional changes during SH-SY5Y neuronal differentiation. However, we also showed significantly increased ID transcripts in postnatal 28 day *Mecp2*$^{-/y}$ mouse brain tissue using qRT-PCR, demonstrating that ID gene dysregulation by MeCP2 deficiency is not limited to the SH-SY5Y neuronal system. The higher level of transcription of all four ID genes in MeCP2 decoy transfected SH-SY5Y neuronal cells and *Mecp2*$^{-/y}$ mice is consistent with the predicted role of MeCP2 as a repressor of genes regulating neuronal maturational differentiation (19). The transient developmental stage specific transcriptional changes of ID genes in *Mecp2*$^{-/y}$ brain observed at P28 (Figure 1B) may explain why ID genes did not appear significant in prior microarray analyses of *Mecp2*$^{-/y}$ brain samples (24).

In addition to changes in the transcripts we also report an increased expression of ID proteins in *Mecp2*$^{-/y}$ mice and human RTT cerebral tissues determined by performing immunofluorescence followed by quantitation by LSC. Interestingly, significantly increased ID protein expression in *Mecp2*$^{-/y}$ was observed at some postnatal time points without a corresponding increase in transcript compared to the controls. Perhaps the developmental stage specific dysregulation of ID transcripts results in long-lived effects on ID protein expression in the brain. We also observed decreased mRNA expression of *Neurod1*, a neurodevelopmentally essential gene target of ID proteins in *Mecp2*$^{-/y}$ mice compared to *Mecp2*$^{+/y}$ controls in all postnatal time points tested. The transient upregulation of ID proteins results in disrupting the auto-regulatory loop and leading to more lasting declines in proteins such as *NEUROD1*. These results suggest that the *Mecp2*-deficient neurons in the mouse model and in RTT patients might become arrested in an immature stage of maturational differentiation

and inappropriately high ID protein levels could either cause or reflect improper neuronal maturation.

Several tissue-specific bHLH transcription factors such as *ASCL1*, *NEUROD1* and *NEUROG1* control the determination and differentiation of neurons in the central and peripheral nervous system (52,53). bHLH proteins dimerize, bind to E-box sequences containing CANNTG and activate transcription of genes (53). The function of bHLH proteins is blocked by ID proteins that are structurally similar to bHLH except that they lack the basic DNA binding domain (38,39,54,55). Four members, ID1 through ID4, have been identified in mammals (38,48,56) as inhibitors of differentiation or inhibitors of DNA binding.

In the absence of ID proteins, bHLH factors function prematurely and terminal differentiation is improperly induced (57). Targeted deletions of all four ID genes have been performed in mouse. Deletion of either *Id1* or *Id3* individually does not lead to an observable phenotype, but when both are inactivated, telencephalic neurogenesis and angiogenesis are greatly perturbed (58). Mice lacking *Id2* are viable, although they have an abnormal immune system and a lactation defect (59,60). Mice lacking *Id4* have a small brain and compromised proliferation of stem cells in the ventricular zone (61).

The role of ID proteins during neuronal differentiation and the overall effect of MeCP2 deficiency on *ID* gene expression are illustrated in the model as shown in Figure 5. In this model, the two-fold increase in MeCP2 expression during neuronal maturation would serve to down-regulate expression of all four ID genes, resulting in the release of more bHLH transcription factors for binding to the E-box of genes involved in neuronal maturational differentiation. Mutation of *MECP2* would therefore increase the levels of ID proteins, thus tipping the balance away from cellular differentiation.

In a recent study, the levels of BDNF protein were reduced in *Mecp2*-deficient mouse brain and deletion of *Bdnf* in *Mecp2*-deficient mice caused an earlier onset of RTT-like symptoms. In contrast, over-expression of conditional *Bdnf* transgene in the *Mecp2*-deficient mice extended lifespan, rescued a locomotor defect, and reversed an electrophysiological deficit (49). Interestingly, within rat *BDNF* promoter III, a Ca^{2+}-responsive E-box element (CaRE2) was identified that binds to two bHLH transcription factors: upstream stimulatory factors 1 and 2 (USF1/2) (50). In addition, a previous study showed that neurotrophins such as BDNF stimulate neuronal differentiation by altering the balance of expression of various bHLH transcription factors (51). Reduced levels of BDNF and increased levels of ID proteins in *Mecp2*-deficent mice might result in lower expression of bHLH proteins, resulting in improper neuronal differentiation.

ID proteins are central to pathways regulating proliferation, differentiation, angiogenesis, migration, invasion and cell-cell interaction. Therefore, by understanding the role of ID proteins during neuronal maturation, they might be therapeutically targeted to reverse the arrest in neuronal maturation seen in RTT and other neurodevelopmental disorders.

MATERIALS AND METHODS

Cell culture and MeCP2 decoy Transfections

SH-SY5Y human neuroblastoma cells (ATCC) were grown in complete minimal essential media with 15 % fetal calf serum in T 175 cm^2 large tissue culture flasks until 70–80 % confluency. The cells were transfected with decoy mixture prepared in serum free MEM containing 3 μl FuGENE 6 (Roche) transfection reagent and 1 μM of either methylated MD or CD, incubated at room temperature for 30 m before addition to the flasks. MeCP2 decoy (MD) and control decoy (CD) were obtained commercially (GeneDetect.com). Both the control

(5' AATCTAGTCTAGACTAGATTA 3') and MeCP2 decoy (5' AATCCGGTCTAGACCGGATTA 3') double-stranded phosphorothioate oligodeoxynucleotides were treated with *Hpa*II methylase (New England Biolabs) (1 U per 1 μg decoy DNA) overnight to methylate the CpG sites. The methylase-treated decoys, MD and CD decoy were digested with *Hpa*II (New England Biolabs) and analyzed by PAGE to confirm methylation. Twelve hours after transfection, cells were treated with 16 nM phorbol 12-myristate 13-acetate (PMA) (Sigma). Total RNA was isolated 48 h after PMA was added using TRIzol reagent (Invitrogen Life technologies) from four different experimental conditions: undifferentiated (UD), differentiated and untransfected (D-UT), differentiated and MeCP2 decoy transfected (D-MD), and differentiated and control decoy transfected (D-CD).

Microarray

Total RNA yield was quantified by spectrophotometric analysis and quality was verified on a gel. A clean up of RNA was performed using RNeasy Mini kit (QIAGEN) before proceeding to cDNA synthesis. 1 μg of RNA under each condition was first reverse transcribed using T7-oligo (dT) promoter primer followed by RNase-H mediated second-stranded cDNA synthesis using One-Cycle cDNA Synthesis kit (Affymetrix). The double stranded cDNA was purified using sample cleanup modules and served as a template in the subsequent *in vitro* transcription (IVT) reaction for complementary RNA (cRNA) amplification and biotin labeling. The biotinylated cRNA targets were cleaned, fragmented and hybridized to Affymetrix HG-U133 plus 2.0 arrays. Detailed procedure of all the steps mentioned above are described in the GeneChip expression analysis technical manual available on the Affymetrix website (http://www.affymetrix.com). A total of 12 array hybridizations were performed consisting of three biological replicates of four experimental conditions each. The hybridizations were performed in a GeneChip hybridization oven 640 and Gene chip fluidics station 450 at the UC Davis Microarray core facility. The image files were obtained using Affymetrix 3000 GeneChip scanner. The raw CEL and DAT files were analyzed using dChip microarray analysis software available at http://biosun1.harvard.edu/complab/dchip/.

Quantitative Real Time RT-PCR (qRT-PCR)

qRT-PCR was performed using a LightCycler rapid thermal cycler system (Roche, Indianapolis, USA) according to the manufacturer's instructions. Primer sequences specific to all four human ID genes and the control house keeping gene, glyceraldehyde 3-phosphate dehydrogenase (*GAPDH*) are listed in supplementary table 6 (S6). The primer sequences for mouse ID genes were obtained from PCR primer bank (62). PCR reactions consisted of 1x DNA master SYBR Green I reaction buffer (Roche), 1.5 mM-2 mM $MgCl_2$, 0.5 μM of primers and 10–20 ng of cDNA. First stranded cDNA was synthesized using reverse transcriptase (Invitrogen) according to the manufacture's protocol from total RNA of SH-SY5Y cells or brain tissue from *Mecp2*$^{+/y}$ and *Mecp2*$^{-/y}$ mice. Detection of the PCR product on LightCycler is carried out at the end of the 72°C extension period. To confirm amplification specificity, the PCR products of each primer pair were subjected to a melting curve analysis. The qRT-PCR data was analyzed using the LightCycler analysis software version 2.0. Final quantification was performed using the comparative CT method (Applied Biosystems) and is reported as n-fold difference relative to an undifferentiated SH-SY5Y control cDNA (UD) or *Mecp2*$^{+/y}$ cDNA of corresponding littermate following normalization to *GAPDH* control gene.

Chromatin immunoprecipitation

Chromatin from human SH-SY5Y neuroblastoma cells from all four conditions (UD, D-UT, D-MD and D-CD) used for microarray experiment was isolated using a procedure previously described (37). ChIP DNA was amplified using primers designed to span 5' CpG islands near

or overlapping the promoter of each *ID* gene and promoter of *SNURF/SNRPN* as a positive control for ChIP assay conditions. Primer sequences are listed in supplementary table 7 (S7).

Mecp2-deficient Mice

Mecp2$^{tm1.1Bird/+}$ (Jackson Laboratories) heterozygous female mice were mated with wild type C57BL/6J mice (Jackson Laboratories) to produce the four possible genotypes. Genotyping was performed using protocols provided by the commercial vendors. Mice were euthanized at different developmental time points (P1 corresponds to day of birth). Whole brain specimens were cut sagitally at the midline using a sterile scalpel and one half was placed in 10 % neutral buffered formalin for 2–3 days and then embedded in paraffin blocks; the other half was placed in TRIzol and stored at −80°C for protein and nucleic acid extractions. Sections of 1 mm were removed from each block followed by sectioning at 5 μm for experimental slides. Hematoxylin and eosin (H & E) slides were prepared for each brain specimen to aid in identification of brain regions. Epitope exposure was carried out as described previously (45).

Mouse Tissue Microarray

Wild type C57BL/6J and *Mecp2*$^{tm1Bird/y}$ tissue for multiple age time points was obtained, fixed and embedded in paraffin and sampled as described above. Mouse tissue array included triplicate 600 μm cores of grey matter from cerebral cortex of six age-matched male mice time points for *Mecp2*$^{+/y}$ and *Mecp2*$^{tm1Bird/y}$ (E 15, P1, P28, P49, P56, and P70).

Human Tissue Microarray

Tissues were received frozen and were fixed, embedded and arrayed as described earlier (46). The human tissue array used contained triplicate 600 μm cores of grey matter from frontal cortex, Broadman area 9, ≤ 30 h PMI. Tissues included on the human array were received from Maryland brain bank and the Harvard brain bank. The array consisted of three cores each of RTT brain samples: RTT 1238 (2y), RTT 1420 (21y), RTT 4312 (24y) and three cores each of three age-matched controls.

Immunofluorescence

Tissue microarrays or whole brain sections were cut into 5 μm sections, placed on glass slides and baked overnight at 56°C. Slides underwent 4 x 5m xylene washes, 2 x 5 m 100 % ethanol washes, dried on a slide warmer (Hybaid) at 50°C, then placed in a 1:10 dilution of DAKO antigen retrieval solution at 95°C for 1 h, cooled to room temperature, and washed for 5 m in 0.2 X SSC. Primary antibodies were diluted in immunofluorescence buffer (IF buffer) (1 X PBS, 0.5 % Tween, 0.01 % Fetal calf serum) added to slides, coversliped and incubated at 37° C for 2 h, washed three times for 5 m in 1 X PBS / 0.5 % Tween. Secondary antibodies diluted in the same IF buffer along with 250 μg/mL RNAse and 3 μg/mL propidium iodide (PI) were then added to slides, coversliped and incubated at 37°C for 1 h followed by 3 x 5 m 1 X PBS / 0.5% Tween washes. Slides were mounted with nuclear counter stain PI (7 μg/ml PI in 50 % glycerol /50% 1X PBS) for analyzing the slides on LSC. Primary antibodies used: anti-ID1 (Santa Cruz, rabbit polyclonal) and anti-ID1 (rabbit monoclonal, kind gift from Dr. Robert Benezra) 1:100, anti-ID2 (Santa Cruz, rabbit polyclonal), anti-ID3 (Santa Cruz, rabbit polyclonal) 1:100, anti-ID4 (Santa Cruz, rabbit polyclonal) 1:100, anti-MeCP2 (Aves, C-terminal, chicken polyclonal) 1:10,000, anti-Histone H1 (Upstate, mouse polyclonal) 1:100. Secondary antibodies used: goat anti-rabbit IgG-Oregon Green (Molecular Probes) 1:100, donkey anti-rabbit IgG-CY5 (Molecular Probes) 1:100, donkey anti-chicken IgY-CY5 (Jackson) 1:100 and goat anti-mouse IgG-Cascade Blue (Molecular Probes) 1:100. Rabbit IgG (Upstate), Chicken IgY (Aves), and Mouse IgG (Upstate) were used at equivalent or higher concentrations than the primary antibodies with the same secondary to test for background levels of staining.

Laser Scanning Cytometry

Slides stained with the above mentioned antibodies were scanned using a Compucyte Laser Scanning Cytometer, as described previously (15,45,46). Settings for voltage, PMT, and threshold were identical between negative control and experimental samples. Nuclei, stained red with PI, were contoured within each core and fluorescence was measured for each nucleus for all channels (red, green, blue and long red). Data was analyzed using Wincyte software from Compucyte.

Supplementary Material

Refer to Web version on PubMed Central for supplementary material.

Acknowledgements

The authors would like to thank Dr. Michael George, Maggie Chiu and Dan Braunschweig for technical assistance. Dr. Edward Jones, Dr. Robert Benezra, Amber Hogart, Karen N. Thatcher, Ravi Nagarajan, Susan Swanberg for valuable comments on the manuscript. Dr. Robert Benezra (Sloan-Kettering, Cancer Biology and Genetics, NY, USA) kindly provided the ID1 antibody. Human tissue samples were generously provided by the Autism Tissue Program, the University of Maryland Brain and Tissue Bank for Developmental Disorders (supported by NIH N01-HD-1-3138), Harvard Brain Tissue Resource Center (supported in part by PHS MH/NS 31862). This work was supported in part by the Rett Syndrome Research Foundation and the NIH (1R01HD/NS41462). S.P was supported by a predoctoral fellowship from the National Alliance for Autism Research.

References

1. Sirianni N, Naidu S, Pereira J, Pillotto RF, Hoffman EP. Rett syndrome: confirmation of X-linked dominant inheritance, and localization of the gene to Xq28. Am J Hum Genet 1998;63:1552–1558. [PubMed: 9792883]
2. Amir RE, Van den Veyver IB, Wan M, Tran CQ, Francke U, Zoghbi HY. Rett syndrome is caused by mutations in X-linked MECP2, encoding methyl-CpG-binding protein 2. Nat Genet 1999;23:185–188. [PubMed: 10508514]
3. Zoghbi HY, Percy AK, Schultz RJ, Fill C. Patterns of X chromosome inactivation in the Rett syndrome. Brain Dev 1990;12:131–135. [PubMed: 2344009]
4. Armstrong DD. Review of Rett syndrome. J Neuropathol Exp Neurol 1997;56:843–849. [PubMed: 9258253]
5. Ellaway C, Christodoulou J. Rett syndrome: clinical update and review of recent genetic advances. J Paediat Child Health 1999;35:419–426.
6. Van den Veyver IB, Zoghbi HY. Methyl-CpG-binding protein 2 mutations in Rett syndrome. Cur Opi Genet Dev 2000;10:275–279.
7. Bird AP, Wolffe AP. Methylation-induced repression--belts, braces, and chromatin. Cell 1999;99:451–454. [PubMed: 10589672]
8. Bird A. DNA methylation patterns and epigenetic memory. Genes Dev 2002;16:6–21. [PubMed: 11782440]
9. Zhao X, Ueba T, Christie BR, Barkho B, McConnell MJ, Nakashima K, Lein ES, Eadie BD, Willhoite AR, Muotri AR, et al. Mice lacking methyl-CpG binding protein 1 have deficits in adult neurogenesis and hippocampal function. Proc Natl Acad Sci U S A 2003;100:6777–6782. [PubMed: 12748381]
10. Hendrich B, Guy J, Ramsahoye B, Wilson VA, Bird A. Closely related proteins MBD2 and MBD3 play distinctive but interacting roles in mouse development. Genes Dev 2001;15:710–723. [PubMed: 11274056]
11. Millar CB, Guy J, Sansom OJ, Selfridge J, MacDougall E, Hendrich B, Keightley PD, Bishop SM, Clarke AR, Bird A. Enhanced CpG mutability and tumorigenesis in MBD4-deficient mice. Science 2002;297:403–405. [PubMed: 12130785]
12. Guy J, Hendrich B, Holmes M, Martin JE, Bird A. A mouse Mecp2-null mutation causes neurological symptoms that mimic Rett syndrome. Nat Genet 2001;27:322–326. [PubMed: 11242117]

13. Chen RZ, Akbarian S, Tudor M, Jaenisch R. Deficiency of methyl-CpG binding protein-2 in CNS neurons results in a Rett-like phenotype in mice. Nat Genet 2001;27:327–331. [PubMed: 11242118]
14. Shahbazian M, Young J, Yuva-Paylor L, Spencer C, Antalffy B, Noebels J, Armstrong D, Paylor R, Zoghbi H. Mice with truncated MeCP2 recapitulate many Rett syndrome features and display hyperacetylation of histone H3. Neuron 2002;35:243–254. [PubMed: 12160743]
15. Braunschweig D, Simcox T, Samaco RC, LaSalle JM. X-Chromosome inactivation ratios affect wild-type MeCP2 expression within mosaic Rett syndrome and Mecp2−/+ mouse brain. Hum Mol Genet 2004;13:1275–1286. [PubMed: 15115765]
16. Balmer D, Goldstine J, Rao YM, LaSalle JM. Elevated methyl-CpG-binding protein 2 expression is acquired during postnatal human brain development and is correlated with alternative polyadenylation. J Mol Med 2003;81:61–68. [PubMed: 12545250]
17. Shahbazian MD, Antalffy B, Armstrong DL, Zoghbi HY. Insight into Rett syndrome: MeCP2 levels display tissue- and cell-specific differences and correlate with neuronal maturation. Hum Mol Genet 2002;11:115–124. [PubMed: 11809720]
18. Akbarian S, Chen RZ, Gribnau J, Rasmussen TP, Fong H, Jaenisch R, Jones EG. Expression pattern of the Rett syndrome gene MeCP2 in primate prefrontal cortex. Neurobiol Dis 2001;8:784–791. [PubMed: 11592848]
19. Zoghbi HY. Postnatal neurodevelopmental disorders: meeting at the synapse? Science 2003;302:826–830. [PubMed: 14593168]
20. Nan X, Campoy FJ, Bird A. MeCP2 is a transcriptional repressor with abundant binding sites in genomic chromatin. Cell 1997;88:471–481. [PubMed: 9038338]
21. Jones PL, Veenstra GJ, Wade PA, Vermaak D, Kass SU, Landsberger N, Strouboulis J, Wolffe AP. Methylated DNA and MeCP2 recruit histone deacetylase to repress transcription. Nat Genet 1998;19:187–191. [PubMed: 9620779]
22. Hendrich B, Bird A. Identification and characterization of a family of mammalian methyl-CpG binding proteins. Mol Cell Biol 1998;18:6538–6547. [PubMed: 9774669]
23. Nan X, Tate P, Li E, Bird A. DNA methylation specifies chromosomal localization of MeCP2. Mol Cell Biol 1996;16:414–421. [PubMed: 8524323]
24. Tudor M, Akbarian S, Chen RZ, Jaenisch R. Transcriptional profiling of a mouse model for Rett syndrome reveals subtle transcriptional changes in the brain. Proc Natl Acad Sci U S A 2002;99:15536–15541. [PubMed: 12432090]
25. Traynor J, Agarwal P, Lazzeroni L, Francke U. Gene expression patterns vary in clonal cell cultures from Rett syndrome females with eight different MECP2 mutations. BMC Med Genet 2002;3:12. [PubMed: 12418965]
26. Colantuoni C, Jeon OH, Hyder K, Chenchik A, Khimani AH, Narayanan V, Hoffman EP, Kaufmann WE, Naidu S, Pevsner J. Gene expression profiling in postmortem Rett Syndrome brain: differential gene expression and patient classification. Neurobiol Dis 2001;8:847–865. [PubMed: 11592853]
27. Chen WG, Chang Q, Lin Y, Meissner A, West AE, Griffith EC, Jaenisch R, Greenberg ME. Derepression of BDNF transcription involves calcium-dependent phosphorylation of MeCP2. Science 2003;302:885–889. [PubMed: 14593183]
28. Martinowich K, Hattori D, Wu H, Fouse S, He F, Hu Y, Fan G, Sun YE. DNA methylation-related chromatin remodeling in activity-dependent BDNF gene regulation. Science 2003;302:890–893. [PubMed: 14593184]
29. Horike S, Cai S, Miyano M, Cheng JF, Kohwi-Shigematsu T. Loss of silent-chromatin looping and impaired imprinting of DLX5 in Rett syndrome. Nat Genet 2005;37:31–40. [PubMed: 15608638]
30. Stancheva I, Collins AL, Van den Veyver IB, Zoghbi H, Meehan RR. A mutant form of MeCP2 protein associated with human Rett syndrome cannot be displaced from methylated DNA by notch in Xenopus embryos. Mol Cell 2003;12:425–435. [PubMed: 14536082]
31. Ballestar E, Ropero S, Alaminos M, Armstrong J, Setien F, Agrelo R, Fraga MF, Herranz M, Avila S, Pineda M, et al. The impact of MECP2 mutations in the expression patterns of Rett syndrome patients. Hum Genet 2005;116:91–104. [PubMed: 15549394]
32. Samaco RC, Hogart A, LaSalle JM. Epigenetic overlap in autism-spectrum neurodevelopmental disorders: MECP2 deficiency causes reduced expression of UBE3A and GABRB3. Hum Mol Genet 2005;14:483–492. [PubMed: 15615769]

33. Nuber UA, Kriaucionis S, Roloff TC, Guy J, Selfridge J, Steinhoff C, Schulz R, Lipkowitz B, Ropers HH, Holmes MC, et al. Up-regulation of glucocorticoid-regulated genes in a mouse model of Rett syndrome. Hum Mol Genet 2005;14:2247–2256. [PubMed: 16002417]
34. Pahlman S, Hoehner JC, Nanberg E, Hedborg F, Fagerstrom S, Gestblom C, Johansson I, Larsson U, Lavenius E, Ortoft E, et al. Differentiation and survival influences of growth factors in human neuroblastoma. Eur J Cancer 1995;31A:453–458. [PubMed: 7576944]
35. Jung BP, Jugloff DG, Zhang G, Logan R, Brown S, Eubanks JH. The expression of methyl CpG binding factor MeCP2 correlates with cellular differentiation in the developing rat brain and in cultured cells. J Neurobiol 2003;55:86–96. [PubMed: 12605461]
36. Klose RJ, Sarraf SA, Schmiedeberg L, McDermott SM, Stancheva I, Bird AP. DNA binding selectivity of MeCP2 due to a requirement for A/T sequences adjacent to methyl-CpG. Mol Cell 2005;19:667–678. [PubMed: 16137622]
37. Thatcher KN, Peddada S, Yasui DH, LaSalle JM. Homologous pairing of 15q11-13 imprinted domains in brain is developmentally regulated but deficient in Rett and autism samples. Hum Mol Genet 2005;14:785–797. [PubMed: 15689352]
38. Benezra R, Davis RL, Lockshon D, Turner DL, Weintraub H. The protein Id: a negative regulator of helix-loop-helix DNA binding proteins. Cell 1990;61:49–59. [PubMed: 2156629]
39. Norton JD, Deed RW, Craggs G, Sablitzky F. Id helix-loop-helix proteins in cell growth and differentiation. Trends Cell Biol 1998;8:58–65. [PubMed: 9695810]
40. Jen Y, Manova K, Benezra R. Expression patterns of Id1, Id2, and Id3 are highly related but distinct from that of Id4 during mouse embryogenesis. Dev Dyn 1996;207:235–252. [PubMed: 8922523]
41. Andres-Barquin PJ, Hernandez MC, Israel MA. Id genes in nervous system development. Histol Histopathol 2000;15:603–618. [PubMed: 10809382]
42. Chae JH, Stein GH, Lee JE. NeuroD: the predicted and the surprising. Mol Cell 2004;18:271–288.
43. Liu KJ, Harland RM. Cloning and characterization of Xenopus Id4 reveals differing roles for Id genes. Dev Biol 2003;264:339–351. [PubMed: 14651922]
44. Ghil SH, Jeon YJ, Suh-Kim H. Inhibition of BETA2/NeuroD by Id2. Exp Mol Med 2002;34:367–373. [PubMed: 12526101]
45. LaSalle JM, Goldstine J, Balmer D, Greco CM. Quantitative localization of heterogeneous methyl-CpG-binding protein 2 (MeCP2) expression phenotypes in normal and Rett syndrome brain by laser scanning cytometry. Hum Mol Genet 2001;10:1729–1740. [PubMed: 11532982]
46. Samaco RC, Nagarajan RP, Braunschweig D, LaSalle JM. Multiple pathways regulate MeCP2 expression in normal brain development and exhibit defects in autism-spectrum disorders. Hum Mol Genet 2004;13:629–639. [PubMed: 14734626]
47. Lopez-Carballo G, Moreno L, Masia S, Perez P, Barettino D. Activation of the phosphatidylinositol 3-kinase/Akt signaling pathway by retinoic acid is required for neural differentiation of SH-SY5Y human neuroblastoma cells. J Biol Chem 2002;277:25297–25304. [PubMed: 12000752]
48. Riechmann V, van Cruchten I, Sablitzky F. The expression pattern of Id4, a novel dominant negative helix-loop-helix protein, is distinct from Id1, Id2 and Id3. Nucleic Acids Res 1994;22:749–755. [PubMed: 8139914]
49. Chang Q, Khare G, Dani V, Nelson S, Jaenisch R. The disease progression of Mecp2 mutant mice is affected by the level of BDNF expression. Neuron 2006;49:341–348. [PubMed: 16446138]
50. Chen WG, West AE, Tao X, Corfas G, Szentirmay MN, Sawadogo M, Vinson C, Greenberg ME. Upstream stimulatory factors are mediators of Ca2+-responsive transcription in neurons. J Neurosci 2003;23:2572–2581. [PubMed: 12684442]
51. Ito H, Nakajima A, Nomoto H, Furukawa S. Neurotrophins facilitate neuronal differentiation of cultured neural stem cells via induction of mRNA expression of basic helix-loop-helix transcription factors Mash1 and Math1. J Neurosci Res 2003;71:648–658. [PubMed: 12584723]
52. Cai L, Morrow EM, Cepko CL. Misexpression of basic helix-loop-helix genes in the murine cerebral cortex affects cell fate choices and neuronal survival. Development 2000;127:3021–3030. [PubMed: 10862740]
53. Lee JE. Basic helix-loop-helix genes in neural development. Curr Opin Neurobiol 1997;7:13–20. [PubMed: 9039799]

54. Norton JD. ID helix-loop-helix proteins in cell growth, differentiation and tumorigenesis. J Cell Sci 2000;113 (Pt 22):3897–3905. [PubMed: 11058077]

55. Ruzinova MB, Benezra R. Id proteins in development, cell cycle and cancer. Trends Cell Biol 2003;13:410–418. [PubMed: 12888293]

56. Sun XH, Copeland NG, Jenkins NA, Baltimore D. Id proteins Id1 and Id2 selectively inhibit DNA binding by one class of helix-loop-helix proteins. Mol Cell Biol 1991;11:5603–5611. [PubMed: 1922066]

57. Yokota Y. Id and development. Oncogene 2001;20:8290–8298. [PubMed: 11840321]

58. Lyden D, Young AZ, Zagzag D, Yan W, Gerald W, O'Reilly R, Bader BL, Hynes RO, Zhuang Y, Manova K, et al. Id1 and Id3 are required for neurogenesis, angiogenesis and vascularization of tumour xenografts. Nature 1999;401:670–677. [PubMed: 10537105]

59. Yokota Y, Mansouri A, Mori S, Sugawara S, Adachi S, Nishikawa S, Gruss P. Development of peripheral lymphoid organs and natural killer cells depends on the helix-loop-helix inhibitor Id2. Nature 1999;397:702–706. [PubMed: 10067894]

60. Mori S, Nishikawa SI, Yokota Y. Lactation defect in mice lacking the helix-loop-helix inhibitor Id2. EMBO J 2000;19:5772–5781. [PubMed: 11060028]

61. Yun K, Mantani A, Garel S, Rubenstein J, Israel MA. Id4 regulates neural progenitor proliferation and differentiation in vivo. Development 2004;131:5441–5448. [PubMed: 15469968]

62. Wang X, Seed B. A PCR primer bank for quantitative gene expression analysis. Nucleic Acids Res 2003;31:e154. [PubMed: 14654707]

Abbreviations

BDNF
: brain derived neurotropic factor

CD
: control decoy (unmethylated oligonucleotide)

ChIP
: chromatin immunoprecipitation

CpG
: Cytosine-phosphate-Guanine (5′-CG-3′)

ID
: inhibitors of differentiation or inhibitors of DNA binding

LSC
: laser scanning cytometer (or cytometry)

MD
: MeCP2 methylated oliconucleotide decoy

MECP2
: methyl-CpG-binding protein 2

PMA
: 2-O-tetradecanoylphorbol-13-acetate

RTT
: Rett syndrome

SNRPN
: small nuclear riboprotein N

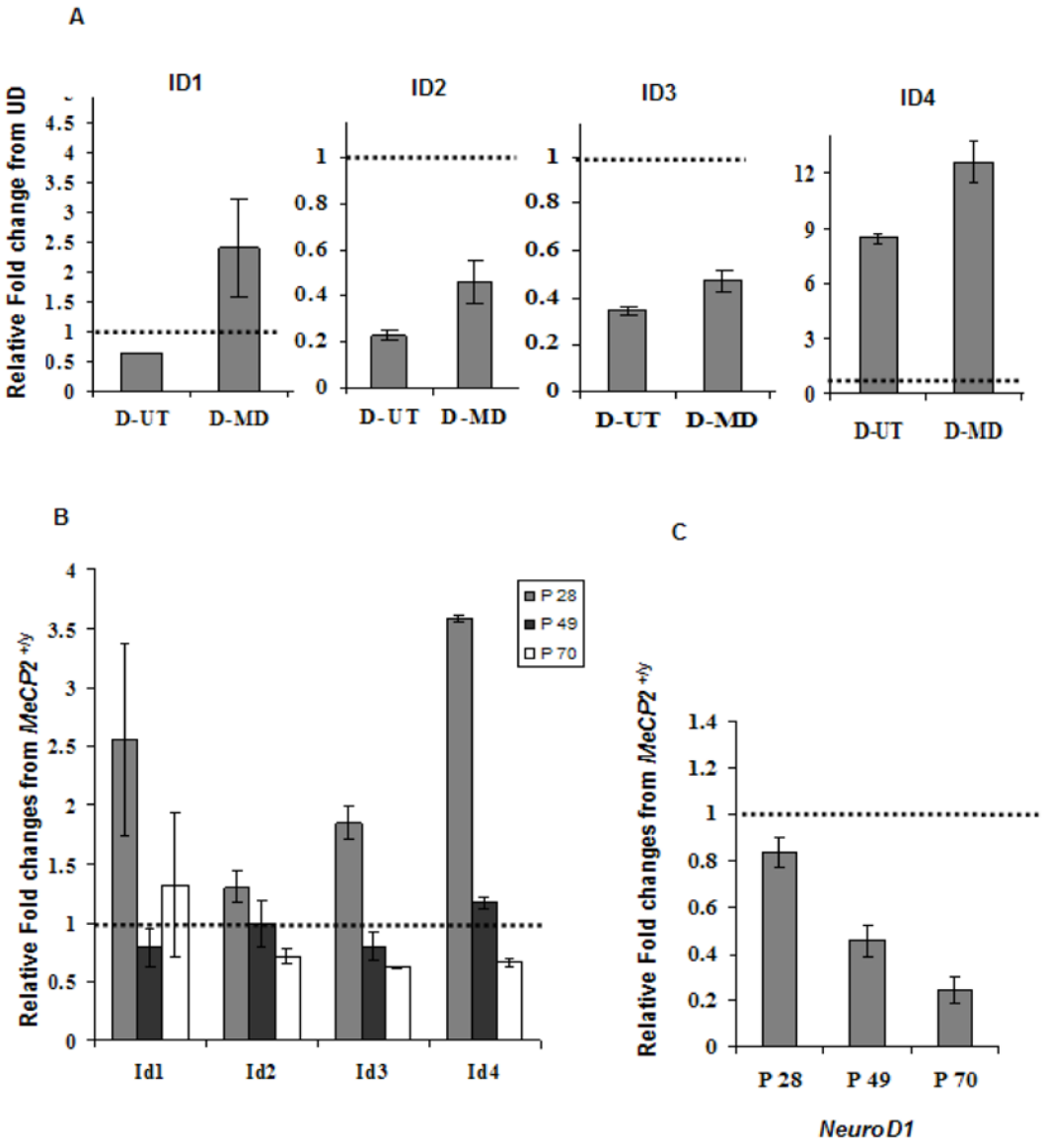

Figure 1. Quantitative RT-PCR results for *ID1-4* in SH-SY5Y, *Mecp2*$^{-/y}$ mouse brain cDNA and *NeuroD1*, a downstream target of ID genes

A, B and C: Graphical representation of all four ID genes qPCR data reflect fold changes relative to the control (set to 1.0, indicated by hatched bar) following normalization of the data to *GAPDH* house keeping control using the comparative CT method. **A)** The qPCR data for *ID1*, *ID2* and *ID3* genes show a decreased expression with differentiation, in untransfected SH-SY5Y cells (D-UT) and increased expression with MeCP2 decoy (D-MD). qPCR data of *ID4* shows an increased expression level following SH-SY5Y differentiation. *ID4* was further increased in the D-MD transfected cells compared to 48 h untransfected (D-UT). Results shown represent mean ± SEM of three replicate experiments. **B)** The qRT-PCR was conducted in cDNA samples from *Mecp2*$^{-/y}$and *Mecp2*$^{+/y}$mice brains. The relative fold change differences for all four ID genes were higher in the *Mecp2*$^{-/y}$ compared to *Mecp2*$^{+/y}$at P28 time point, and reached significance by t-test for *Id3* and *Id4* ($P < 0.05$). No increase in cDNA was observed at later time points (P49 and P70). **C)** The qRT-PCR results on a downstream target of ID genes, *NeuroD1*, showed lower expression in all three postnatal time points (P28, P49 and P70)

in *Mecp2*$^{-/y}$ brain compared to the *Mecp2*$^{+/y}$ control brain, with significantly reduced expression at P49 and P70 by t-test ($P \leq 0.05$). Each time point in bar graphs B and C represents mean ± SEM of three replicate experiments from two pairs of mice per time point.

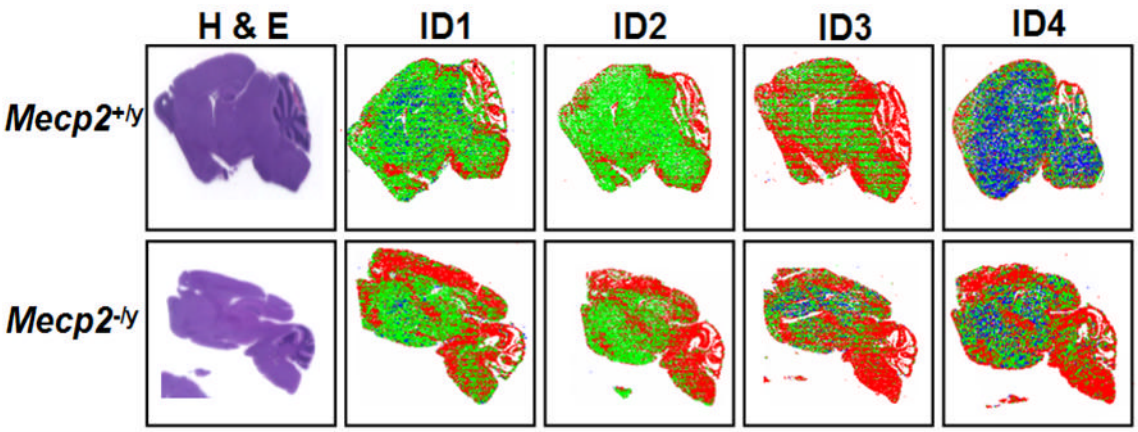

Figure 2. Increased ID protein expression changes in *Mecp2*-deficient mice model detected by immunofluorescence and LSC

Immunofluorescence followed by analysis on LSC was performed on postnatal day 28, 5 μm sagittal brain sections of three pairs of *Mecp2*$^{-/y}$ and *Mecp2*$^{+/y}$ mice using antibodies recognizing ID1, ID2, ID3 and ID4. Representative LSC image showing protein expression differences in multiple regions of the brain of *Mecp2*$^{-/y}$ mice compared to *Mecp2*$^{+/y}$ controls for all four ID proteins. Each pixel represents individual nuclei colored blue (negative), green (low) or red (high) based on max pixel fluorescence histograms. For each section, the hemotoxylin and eosin (H&E) stained parallel slide was used to determine the tissue localization of cells and gating of individual brain regions for quantitative data shown in Table 3.

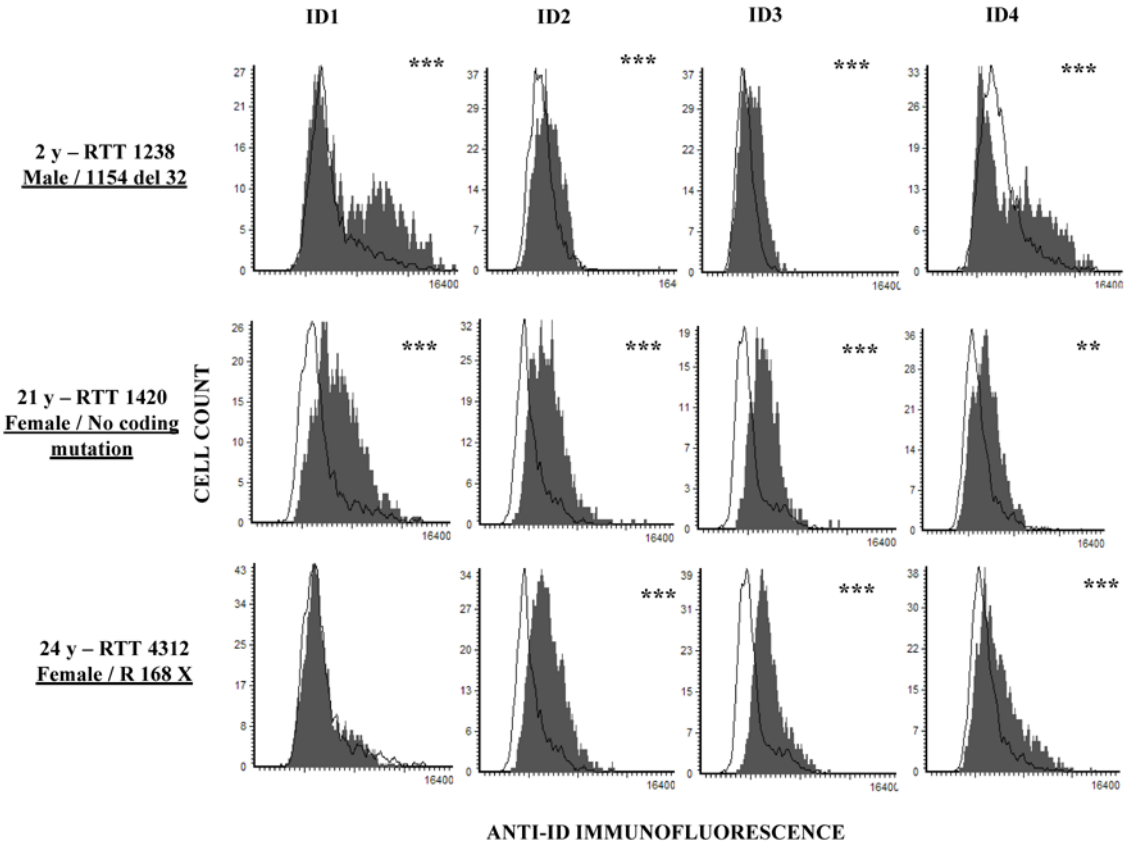

Figure 3. Increased ID protein expression changes in RTT cerebrum detected by immunofluorescence and LSC

Immunofluorescence using antibodies recognizing ID1-4 was performed on postmortem cerebral cortex samples from one male and two female RTT samples with and without *MECP2* coding mutations (filled, grey histograms) and age-matched controls (open, black histogram) arranged on a tissue microarray. Expression of all four ID proteins was significantly increased in RTT brain samples compared to the controls. In contrast, histone H1 expression was not significantly changed (data not shown). Significance was determined using chi-square from two replicate experiments and the *P* values are denoted by asterix on the top right corner of each histogram. (* $P \leq 0.05$, ** $P \leq 0.005$, *** $P \leq 0.0005$).

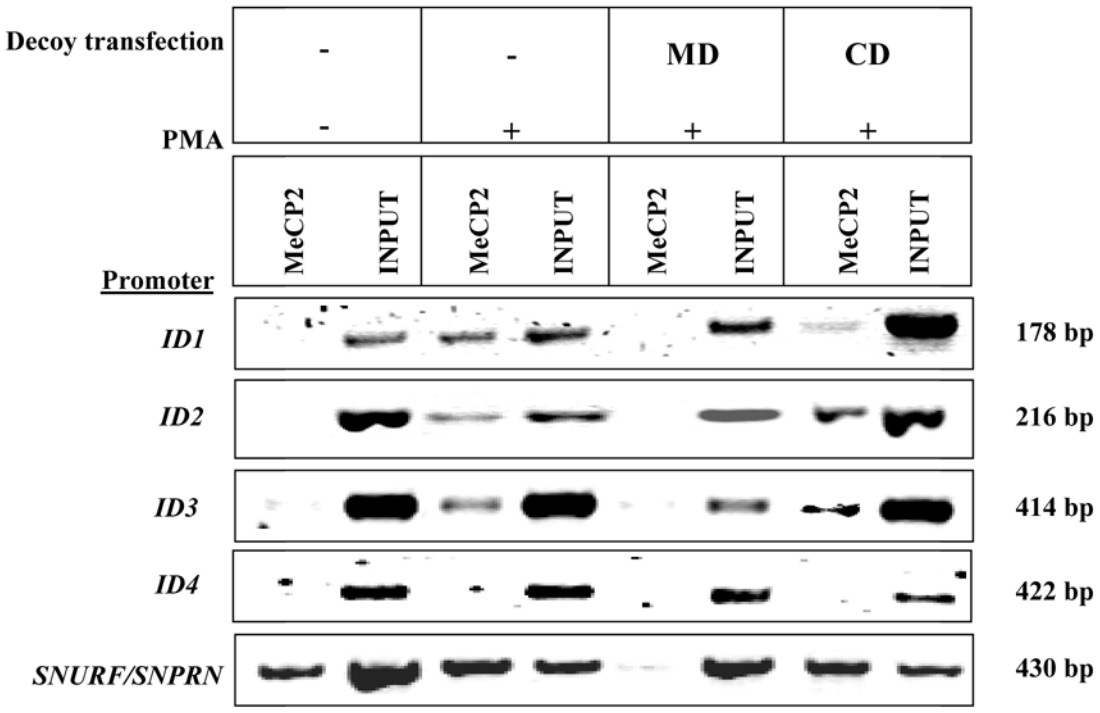

Figure 4. Chromatin Immunoprecipitation (ChIP) analysis of MeCP2 binding to *ID1, ID2 and ID3* promoters

Representative gel of PCR products using primers specific to each of the ID gene promoter following ChIP with C-terminal MeCP2 reactive antibody. The total DNA isolated from chromatin prior to IP (Input) was used as a positive control. The ChIP results show binding of MeCP2 near or within the promoter of *ID1*, *ID2* and *ID3* in differentiated SH-SY5Y cells (D-UT) and control decoy transfected cells (D-CD). For *ID4*, binding of MeCP2 was not observed near or within the promoter region assayed. Additionally, the binding of MeCP2 to *SNURF/SNRPN* promoter is shown as a positive control for ChIP assay conditions.

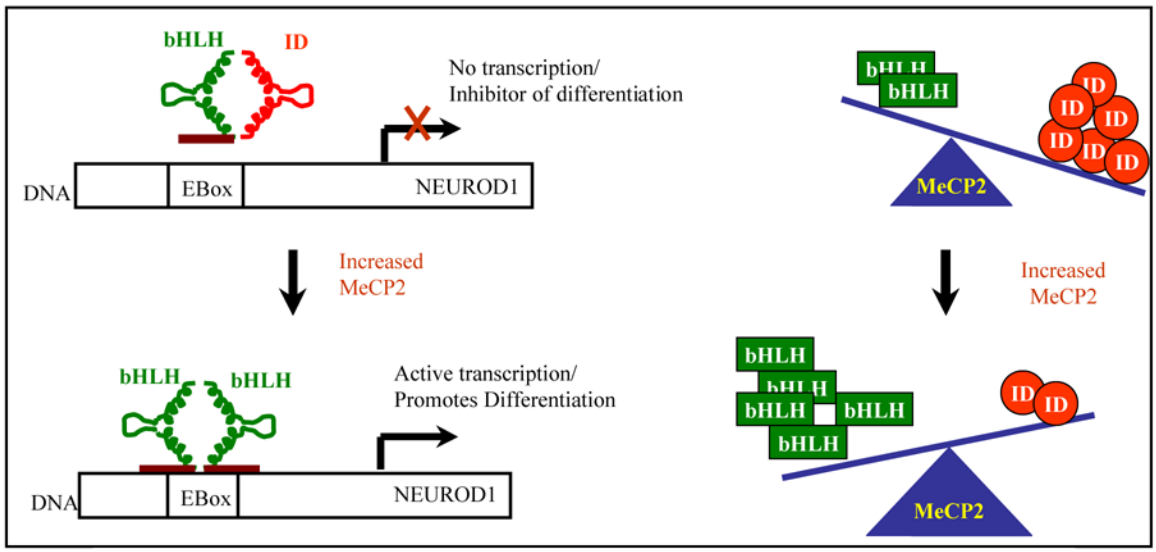

Figure 5. Model for role of ID proteins in regulating neuronal maturational differentiation

In immature neurons with high expression of ID proteins, heterodimers of bHLH-ID prevent DNA binding and expression of differentiation associated genes like *NEUROD1*. Upon neuronal maturation, elevated levels of MeCP2 repress the expression of ID genes, resulting in functional bHLH-bHLH dimers that can bind to E-box DNA sequences and activate transcription of differentiation associated genes such as *NEUROD1*, *ASCL1* and *NEUROG1*.

Table 1

Selection for primary target genes of MeCP2 during SH-SY5Y cell differentiation

Criteria for Selection	# of Probe sets	# of Genes
Significant ($p \leq 0.05$) AND increased by ≥ 2.0 fold change in expression upon differentiation **(UD vs. D-UT)**	261	183
Out of 183 genes, genes significant ($p \leq 0.05$) AND increased by ≥ 1.2 fold change in expression with MeCP2 decoy NOT control decoy	14	12
Out of 183 genes, genes significant ($p \leq 0.05$) AND decreased by ≥ 1.2 fold change in expression with MeCP2 decoy NOT control decoy	10	8
Significant ($p \leq 0.05$) AND decreased by ≤ 2.0 fold change in expression upon differentiation **(UD vs. D-UT)**	60	45
Out of 45 genes, genes significant ($p \leq 0.05$) AND increased by ≥ 1.2 fold change in expression with MeCP2 decoy NOT control decoy	5	4
Out of 45 genes, genes significant ($p \leq 0.05$) AND decreased by ≥ 1.2 fold change in expression with MeCP2 decoy NOT control decoy	0	0

Table 2

All members of the ID gene family are significantly increased by MeCP2 decoy

			Undifferentiated vs. Differentiated and Untransfected (UD vs. D-UT)		Differentiated and Untransfected vs. MeCP2 decoy transfected (D-UT vs. D-MD)	
Gene Description	**Gene Symbol**	**Chromosomal Location**	**Fold Change**	**P value**	**Fold Change**	**P value**
Inhibitor of DNA binding 1	*ID1*	20q11	−2.91	0.00054	1.45	0.00406
Inhibitor of DNA binding 2	*ID2*	2p25	−3.22	0.00166	1.52	0.03498
Inhibitor of DNA binding 3	*ID3*	1p36.13-p36.12	−2	0.00099	1.25	0.01702
Inhibitor of DNA binding 4	*ID4*	6p22-p21	2.53	0.00152	1.71	0.03737

Table 3

Significant expression differences of ID1, ID2, ID3 and ID4 proteins in different brain regions of postnatal day 28 (P28) *Mecp2*$^{-/y}$ mice compared to the *Mecp2*$^{+/y}$ mice

	Pair 1				Pair 2				Pair 3			
	Mecp2$^{+/y}$		*Mecp2*$^{-/y}$		*Mecp2*$^{+/y}$		*Mecp2*$^{-/y}$		*Mecp2*$^{+/y}$		*Mecp2*$^{-/y}$	
Brain Region	**Mean ± SEM**	**Cell #**	**Mean ± SEM** [c]	**Cell #**	**Mean ± SEM**	**Cell #**	**Mean ± SEM** [c]	**Cell #**	**Mean ± SEM**	**Cell #**	**Mean ± SEM** [c]	**Cell #**
Inhibitor of differentiation 1-ID1 [a]												
Whole brain	6308 ± 8	52657	7435 ± 9***	43790	5497 ± 8	51079	5852 ± 8***	54931	5057 ± 7	48906	6018 ± 7***	39591
Cerebellum	7466 ± 30	6733	8250 ± 29***	4679	6095 ± 24	4504	7231 ± 30***	5873	5998 ± 24	4705	6807± 32***	2974
Cerebrum	5946 ± 18	7588	8540 ± 26***	5908	4833 ± 13	10331	5548 ± 18***	8179	4677 ± 20	7547	6191 ± 20***	6504
Medulla oblongata & Pons	6716 ± 19	10831	7512 ± 17**	9295	6535 ± 20	11919	6242 ± 21	8790	5802 ± 16	9790	6194 ± 19***	6192
Thalamus & Hypothalamus	6068 ± 21	5256	6459 ± 21***	5766	4855 ± 21	4407	5801 ± 23***	6926	4558 ± 15	6456	5776 ± 17***	5094
Hippocampus	5373 ± 20	4760	6660 ± 26***	3569	4572 ± 19	3510	5230 ± 28***	3567	4704 ± 24	3536	6026 ± 30***	2206
Inhibitor of differentiation 2-ID2 [b]												
Whole brain	7684 ± 9	47590	10303 ± 10***	44703	6792 ± 9	51113	8025 ± 10***	51882	8203 ± 9	48244	8720 ± 9***	41791
Cerebellum	9264 ± 31	6493	11948 ± 24***	5208	7451 ± 29	4368	8679 ± 32***	5451	9423 ± 27	4731	9760 ± 31***	3385
Cerebrum	7427 ± 22	5579	11581 ± 34***	4023	6206 ± 20	8494	8130 ± 24***	8093	7664 ± 23	7753	8172 ± 20***	6488
Medulla oblongata & Pons	7772 ± 22	9403	10081 ± 19***	7780	7486 ± 19	12563	7987 ± 25***	8805	9143 ± 20	9661	9211 ± 23^{NS}	7911
Thalamus & Hypothalamus	7480 ± 26	4322	8667 ± 24***	4913	6540 ± 27	5013	8168 ± 27***	6286	7807 ± 23	5587	8064 ± 19***	5813
Hippocampus	6793 ± 24	4210	9519 ± 42***	2119	5921 ± 29	3144	8110 ± 48***	2611	8052 ± 34	2914	8667 ± 33***	2614
Inhibitor of differentiation 3 -ID3 [b]												
Whole brain	5727 ± 8	37924	6625 ± 8***	43220	5265 ± 7	48152	5400 ± 8***	52891	5475 ± 7	48680	6656 ± 7***	37111
Cerebellum	6399 ± 22	4146	7374 ± 23***	4281	5891 ± 25	3907	6418 ± 25***	5869	6158 ± 22	4800	7600 ± 41***	1727
Cerebrum	7054 ± 21	7549	6648 ± 22	8482	5407 ± 18	8940	4892 ± 16	9054	5185 ± 23	6590	6816 ± 18***	6851
Medulla oblongata & Pons	6762 ± 15	8616	7070 ± 16***	8956	5398 ± 14	11080	5801 ± 20***	9235	6114 ± 15	10348	6812 ± 15***	8285
Thalamus & Hypothalamus	5612 ± 20	3947	6451 ± 25***	4331	5058 ± 20	4219	5375 ± 22***	6585	5127 ± 16	6560	6351 ± 16***	5117
Hippocampus	4589 ± 22	2725	5619 ± 24***	3595	4864 ± 25	3005	5019 ± 29*	3180	5180 ± 29	3287	6861 ± 26***	2495
Inhibitor of differentiation 4 -ID4 [b]												
Whole brain	5247 ± 7	40365	6437 ± 8***	41372	5328 ± 8	47817	5900 ± 9***	50306	4840 ± 7	49215	6061 ± 7***	40687
Cerebellum	5762 ± 23	4189	6886 ± 21***	5167	5634 ± 18	4195	6738 ± 21***	6231	5572 ± 20	5941	7291 ± 34***	2431
Cerebrum	5476 ± 14	9279	6794 ± 21***	8203	5176 ± 19	8749	5618 ± 21***	8022	4768 ± 19	8157	6289 ± 16***	9627
Medulla oblongata & Pons	5290 ± 14	9192	6951 ± 15***	10192	6206 ± 23	10537	5812 ± 23	8560	5144 ± 16	9198	6063 ± 16***	7732
Thalamus & Hypothalamus	5016 ± 18	4912	5997 ± 21***	4631	5293 ± 25	5204	5702 ± 33***	6995	4446 ± 17	5432	5504 ± 16***	5860
Hippocampus	4896 ± 18	3618	5651 ± 22***	3726	5096 ± 26	3517	5790 ± 30***	3331	4706 ± 25	2635	6048 ± 27***	2441

[a]- ID1 rabbit monoclonal antibody used is provided by Dr. Robert Benezra.

[b]- ID2, ID3, ID4 rabbit polyclonal antibodies obtained from commercially available source (Santa Cruz Biotechnologies, Inc).

[c]- Significance determined by chi-square and P values denoted by asterix.

* $P \leq 0.05$,

** $P \leq 0.005$,

*** $P \leq 0.0005$.

Table 4

Significant expression differences of ID1, ID2, ID3 and ID4 proteins in the frontal cortex of *Mecp2*$^{-/y}$ mice compared to the *Mecp2*$^{+/y}$ mice at various developmental time points

		Mecp2$^{+/y}$		*Mecp2*$^{-/y}$	
Brain Region	**Age (days)**	**Mean ± SEM**	**Cell #**	**Mean ± SEM** [b]	**Cell #**
Inhibitor of differentiation 1 - ID1 [a]					
Frontal Cortex	E 15	4381 ± 59	848	5026 ± 96**	488
	P 7	4964 ± 19	2951	5639 ± 23***	2866
	P 28	4479 ± 28	1943	5015 ± 39**	1016
	P 49	4441 ± 25	2581	5112 ± 43***	1070
	P 56	3750 ± 20	2054	3876 ± 21	1918
	P 70	4643 ± 43	1454	5097 ± 37**	2046
Inhibitor of differentiation 2 - ID2 [a]					
Frontal Cortex	E 15	4432 ± 51	859	5078 ± 65**	519
	P 7	5100 ± 32	1090	6152 ± 44***	1076
	P 28	4387 ± 44	2122	4622 ± 48**	947
	P 49	3457 ± 25	1189	4228± 58***	523
	P 56	3282 ± 18	1064	3552 ± 26**	990
	P 70	4397 ± 52	699	5665 ± 63***	1002
Inhibitor of differentiation 3 - ID3 [a]					
Frontal Cortex	E 15	4052 ± 48	1130	3917 ± 62	481
	P 7	4577 ± 38	2464	5211 ± 38***	2032
	P 28	6437 ± 74	627	6494 ± 60	532
	P 49	6386 ± 82	561	6687 ± 86	376
	P 56	5034 ± 28	1122	5390 ± 40*	699
	P 70	6295 ± 70	581	6773 ± 64*	737
Inhibitor of differentiation 4 - ID4 [a]					
Frontal Cortex	E 15	6568 ± 84	817	6295 ± 123	450
	P 7	5151± 45	566	5347 ± 43	650
	P 28	4095 ± 38	1062	4784 ± 44*	516
	P 49	3653 ± 34	605	4806 ± 41**	602
	P 56	3645 ± 36	436	4148 ± 35**	579
	P 70	4607 ± 60	438	5722 ± 55***	557

[a] - ID1, ID2, ID3, ID4 rabbit polyclonal antibodies obtained from commercially available source (Santa Cruz Biotechnologies, Inc).

[b] - Significance determined by chi-square and P values denoted by asterix.

* $P \leq 0.05$,

** $P \leq 0.005$,

*** $P \leq 0.0005$.